A critical study on the Optical and morphological characteristics of Aluminium doped zinc oxide thin films

Richa Sharma[a], Fouran Singh[b] and J M S Rana[a]

[a] Department of Physics, H.N.B Garhwal University, SRT Campus Badshahi Thaul, Tehri Garhwal 249199, India

[b] Materials Science Group, Inter University Accelerator Centre, Aruna Asaf Ali Marg New Delhi 110 067, India

Abstract: Aluminium doped ZnO (AZO) thin films were deposited by sol-gel spin coating method on corning glass substrate. The effect of Al concentration (1.5%, 2% and 2.5 mol% AZO) and annealing temperature (500ºC, 600ºC and 700ºC) on structure, morphology and optical properties of the thin films have been studied by X-Ray diffraction, field emission scanning electron microscopy (FE-SEM) and UV-VIS spectroscopy, respectively. All the deposited thin films show the crystallite growth in c-axis (002) orientations with hexagonal wurtzite structure. An enhancement in crystallinity was observed with increasing annealing temperature. The crystallite size has been found to decrease with an increase in Al concentration and these results are further correlated with SEM investigations. The crystallite size and lattice constant calculation reveal nano crystalline nature of the particles. SEM images give the morphology of the film that consists of uniform spherical grains. An optical transmittance of 90% has been attained for 2.5% AZO films annealed at 700℃ in oxygen environment. The optical studies show a shift in absorption edge from 370 nm to 350 nm with increasing annealing temperature. Blue shift in the optical band gap is witnessed with rise in dopant concentration and increasing annealing temperature. The electrical transport properties are studied by two probe method.

Key Words: Transparent conducting oxides (TCOs); ZnO:Al (AZO); optical band gap.

1. INTRODUCTION

There are wide range of potential applications of Transparent conducting oxide (TCO) films in various fields such as liquid crystal displays, thin film transistors, optical sensors and organic light-emitting devices etc (Park et al., 2009; Pramod & Pandey, 2014; Yu, Yang, Chen, Tao, & Liu, 2016). The rapid evolution of technology enables feasibility of these future technologies using Indium tin oxide (ITO) for the TCO applications. Moreover, the properties such as high transmittance, in visible region, and low resistivity make ITO the widely used candidate. However, the de-merits such as high cost, toxic nature and chemical instability intrigued the researchers to investigate for a candidate to overcome these barriers. Among all TCOs, zinc oxide (ZnO) comes out to be a good alternative to ITO. ZnO, the II-VI semiconductor, is an abundant, low cost and non-toxic in nature compared to ITO and is also the most extensively investigated material with a wide direct band gap(Hosford, 2013). The type of conductivity of ZnO can be understood in view of native donor defects, vacancies which are created by oxygen and zinc-interstitials results in n-type conductivity in ZnO. However, the n-type or p-type conductivity can be altered by doping or by creating controlled defects into the lattice(Gautam, Singh, Kumar, & Singh, 2015; Look & Hemsky, 2000). Although ZnO is an impressive metal-oxide semiconductor with a good optical and electrical properties, these can be easily modified by doping with different elements and varied concentration. It has been established that ZnO doped with III group impurities, such as Al, Ga, B, Mn, and Cr, modify the optical and transport properties of ZnO thin films(Fiat Varol, Babür, Çankaya, & Kölemen, 2014; Nunes, Fortunato, Vilarinho, & Martins, 2001; Venkataraj et al., 2007). Among all these dopants Al emerges to be the most promising element, as it modifies ZnO

in such a way that it can suitably replace ITO. An already reported study suggested that Al doped ZnO (AZO) thin films exhibit improved optical and electrical properties in addition to better thermal, chemical and mechanical properties (Pat et al., 2017; Srinatha, Raghu, Mahesh, & Angadi, 2017). The manipulations of various properties of ZnO are attributed to changes in the defects environment by Al doping in ZnO. Different chemical and physical fabrication techniques are reported for the preparation of high quality AZO thin films, including sol-gel spin coating(Li, Yang, & Zhu, 2017; Srinatha et al., 2017), RF magnetron sputtering(Pat et al., 2017), pulsed laser deposition (PLD)(Kaur, Mitra, & Yadav, 2015), spray pyrolysis(Barón-Miranda et al., 2017) and chemical vapour deposition(Thandavan, Gani, Wong, & Nor, 2015) (CVD). In the present work, we adopted sol-gel spin coating technique for undoped ZnO and AZO thin films deposition. This technique imbibes low cost, large area and simple fabrication of the thin films(Brinker & Scherer, 1990). We aim at to investigate the optical, structural, microstructural and electrical properties of ZnO and AZO thin films with different Al concentration and annealing temperatures. Post thermal treatment is a good tool that modifies the various properties in ZnO thin film by removal of defects and thus resulting in the emancipation of internal stress(Singh, Singh, Kumar, & Mehra, 2011).

2. EXPERIMENTAL DETAILS

The sol-gel spin coating method is employed for the fabrication of undoped ZnO and AZO thin films with Aluminium concentration of 1.5, 2 and 2.5 mol%. The material chosen for sol preparations were Zinc acetate dihydrate (Zn $(CH_3COO)_2$ $2H_2O$), Aluminium Chloride Hydrate ($AlCl_3 \times H_2O$), 2- methoxyethanol and mono-ethanol-amine (MEA). The source Zinc acetate is dissolved in solvent 2- methoxyethanol for undoped ZnO sol. To obtain sol for AZO, Aluminium Chloride Hydrate is added as dopant to the mixture in stoichiometric amount for different doping percentage. The mixture solution was then stirred for 60 min in magnetic stirrer. For obtaining the clear homogeneous solution MEA (stabilizer) is added drop wise. The as prepared solution was aged at room temperature for 72 hours. The molar concentration of zinc acetate was 0.4 M and the molar ratio of zinc acetate and MEA was maintained at 1:1. The corning glass substrate were thoroughly cleaned with a solution of DI water and acetone in an ultrasonic cleaner for 10 min and then blow dried with air blower. The deposition of undoped, 1.5, 2 and 2.5 mol% AZO were done by using spin coater at the speed of 2800 rpm for 30 sec. The film was then heated at 350˚C for 10 min on hot plate, this process evaporate the solvent and organic residuals. The two step process of coating and heating was repeated 12 times to obtain the desired film thickness. The films are then annealed at three different temperature i.e. 500˚C, 600˚C and 700˚C in the oxygen environment for 1h microprocessor controlled tubular furnace. The flow rate of oxygen was fixed for all the prepared samples.

The crystallinity and structure of undoped ZnO and AZO thin films have been characterized at room temperature by using a glancing angle X-ray diffractometer (GAXRD), using Bruker D8 diffractometer with Cu-Ka X-ray (l-1.54 Å) for 2θ range from 20 to 80 with a scan rate of 0.2/m. The microstructure and morphological investigations were done by a Scanning Electron Microscopy (SEM). Optical transmittance and absorbance spectra from 200 to 800 nm wavelength range were recorded using Hitachi UV 3300 double beam spectrometer. The electrical transport properties are studied by two probe method using Keithley nanovoltmeter setup.

3. RESULTS AND DISCUSSIONS

3.1. Structural studies

The XRD measurement are carried out for investigating the structural features of undoped ZnO and AZO thin films on the corning glass substrates. Fig (a) and (b) depicts the recorded XRD pattern of the films. All the samples feature poly crystalline hexagonal structure in harmony with the Joint Committee of Power Diffraction Standards (JCPDS) card No. 36-1451. Fig (a) shows the XRD pattern of thin films annealed at 700ºC in oxygen environment with different dopant concentration. Accordingly, the growth in all of the samples is along (100), (002), (101) and (103) planes but with preferred orientation along (002) plane. The (002) differential peak is identified for the hexagonal wurtzite ZnO with c-axis orientation. The orientation of the crystal growth is always in the lowest surface energy direction. In ZnO crystal (002) c-axis orientation has the lowest surface energy density. The diffraction pattern reveals that the crystal growth is not affected by the Al doping upto 2% but for 2.5% AZO thin films lower c-axis orientation is observed. The absence of other impurity phases even upto 2.5% Al doping confirms that the dopant does not alters the crystal structure. This indicates high purity of produced samples and that the Al is well substituted in Zn site. The diffraction pattern reveals a difference in the peak width and their intensities but the overall crystal structure of AZO thin films remain all the same as that of undoped ZnO thin film structure. It is observed that (002) peak intensity increases with increasing Al concentration upto 2% and then for 2.5% AZO thin films the intensity falls drastically. This decrease points out toward the structure degradation.

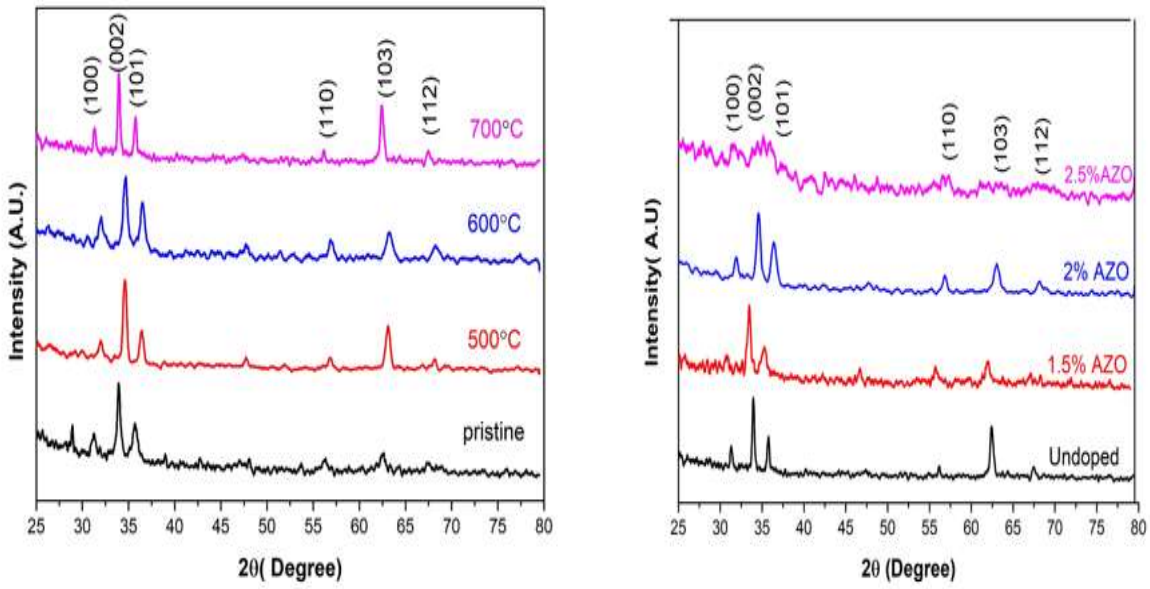

Figure 1: XRD pattern of thin films (a) undoped ZnO thin films annealed at different annealing temperature (b) increasing Al concentration annealed at 700ºC.

This degradation assert the fact that an excess increase in dopant concentration depreciates the crystallinity of films. Analogous results are observed by S.Y. Kuo et al.(Kuo et al., 2006). Thus, thin films with lower Al concentration possess good crystal structure in comparison to thin films with higher Al concentration. The effect of annealing temperature featured well in Fig (b) of undoped ZnO at different annealing temperatures. It is observed

that the increased annealing temperature promotes the (002) orientation. The increasing peak intensity reflects that the rise in annealing temperature leads to the improvement in crystallinity in films. However, this improvement in crystallinity may reduce the optical scattering from grain boundaries stemming from the minimisation of the internal stress in the thin films.

Table1: Different parameters calculated from XRD pattern

Sample	FWHM (002)	Crystallite size D(nm)	Dislocation density δ (10^{14} lines m^{-2})	Strain ε(10^{-4})	Stress σ(GPa)	Lattice parameters	
						a=b (Å)	c(Å)
Undoped ZnO	0.297	27.90	12.77	41.85	-0.975	3.246	5.206
1.5 AZO	0.434	19.16	27.24	61.13	-1.424	3.255	5.207
2AZO	0.477	17.45	32.84	66.89	-1.558	3.238	5.190
2.5AZO	0.380	21.89	20.87	52.75	-1.229	3.251	5.132

Further to estimate different thin film parameters, highest intense peak, (002) diffraction peak is used. The pattern reveals that the value of full width half maximum (FWHM) of peak (002) increases with an increase in the aluminium concentration up to 2% AZO. This increase in FWHM, with Al concentration indicates the decrease in crystallite size, which is calculated by employing Scherrer's formula (1) as following(Srinatha et al., 2017)

$$D = \frac{K\lambda}{\beta cos\theta} \quad (1)$$

Where, K=0.9 is Scherer's constant which depends on the shape of crystallite, λ=1.5418 Å, is X-ray wavelength for Cu Kα target, β is FWHM for (002) peak and θ is the Bragg's angle (half of the peak position angle). The calculated values of crystallite size are found to decrease with increase in Al dopant concentration (organized in Table 1). The data thus obtained reveals that all the thin films formed consist of nano sized structures. Similar results have been observed by other research groups(Srinatha et al., 2017; Yilmaz et al., 2016). Such structures can be attributed to smaller ionic radius of Al^{3+}(0.54 Å) as compared to Zn^{2+} (0.74 Å) in tetrahedral symmetry. With an increase in annealing temperature from the deposition to 700℃ the values of crystallite size D tends to increase from 15.97nm to 27.90nm. This rise in D can be due to larger grain growth induced by extra energy supplied through the higher annealing temperature causing the merging process of smaller grains(Malek et al., 2015).

The lattice constant a and c are calculated by the following formulae(Kaur et al., 2015)

$$a = \frac{\lambda}{\sqrt{3}sin\theta_{(100)}} \qquad c = \frac{\lambda}{sin\theta_{(002)}} \qquad (2)$$

The calculated values of lattice parameters are found to be consistent with $a = 3.2498$Å and $c = 5.2066$Å according to JCPDS card no. 36-1451. The observed changes in these parameters indicate towards the effective substitution of the Al^{3+} ion at the Zn^{2+} site in the ZnO lattice. The changes can be attributed to the induced stress due to difference in the ionic radius of Al and ZnO. The dislocation density (δ)has been calculated by employing the following formula(Yilmaz et al., 2016)

$$\delta = \frac{1}{D^2} \qquad (3)$$

It is defined as the length of the dislocation lines per unit volume and give details about the degree of defects in crystal structure. The microstrain (ε) in the films have been estimated using following formula(Yilmaz et al., 2016):

$$\varepsilon = \frac{\beta}{4tan\theta} \qquad (4)$$

Where, β is FWHM and θ is the Bragg's angle. The calculated values of dislocation density δ and microstrain ε are tabulated in Table 1. Both the values show a tendency to rise with Al concentration upto 2% and then decrease for 2.5% Al concentration. This trend may be attributed to decrease in crystallite size and structural disorders in the crystal structure due to excess Al contribution. Similar results have been observed by N.Srinatha et al.(Srinatha et al., 2017). The differences in the ionic radius of Al and Zn generates a stress in the AZO thin films which can be classified as intrinsic and extrinsic. The defects and impurities in the crystal are responsible for the intrinsic stress while the growth parameters, mismatch in lattice and difference in the thermal coefficient of substrate and film give rise to the external stress.(Joshi et al., 2016) The c-axis stress in the AZO thin films is calculated by employing the biaxial strain model(Jo, Kim, & Koh, 2018):

$$\sigma = \frac{2c_{13}^2 - c_{33}(c_{11} - c_{12})}{2c_{13}} \times \varepsilon \qquad (5)$$

Where the elastic constants of single crystal, $c_{11}, c_{12}c_{13}$and c_{13} have the values 208.8, 114.7, 104.2 and 213.8 respectively. Equation (5) can be simplified to

$$\sigma = -233 \times \varepsilon(GPa).$$

The calculated values of stress are tabulated in Table1. The negative values of stress indicate intrinsic stress in the films which is compressive in nature. The estimated decrement in the stress values inferred the improvement in crystallinity of the films with increasing Al concentration.

3.2. Morphological studies

The morphological studies shows that the sol-gel spin coated thin films have spherical grain which are uniformly distributed and covered the substrate surface without any crack. The FE-SEM micrographs of undoped ZnO and AZO thin films with increasing Al dopant concentration annealed at 500˚C are shown in Fig2. The FE-SEM images clearly indicate that the dopant concentration had great influence on the surface morphology. Round shaped structures of different sizes are observed in the thin films. The observed c-axis preferred orientation originates the round shape structure. These results were expected and are in harmony with the observed XRD results with (002) preferred growth orientation. The 1.5% and 2% AZO thin films exhibit porous structure. The increase in aluminium concentration reduced the particle size and brought the denser microstructure in 2.5% AZO thin films as compared to that of undoped ZnO.

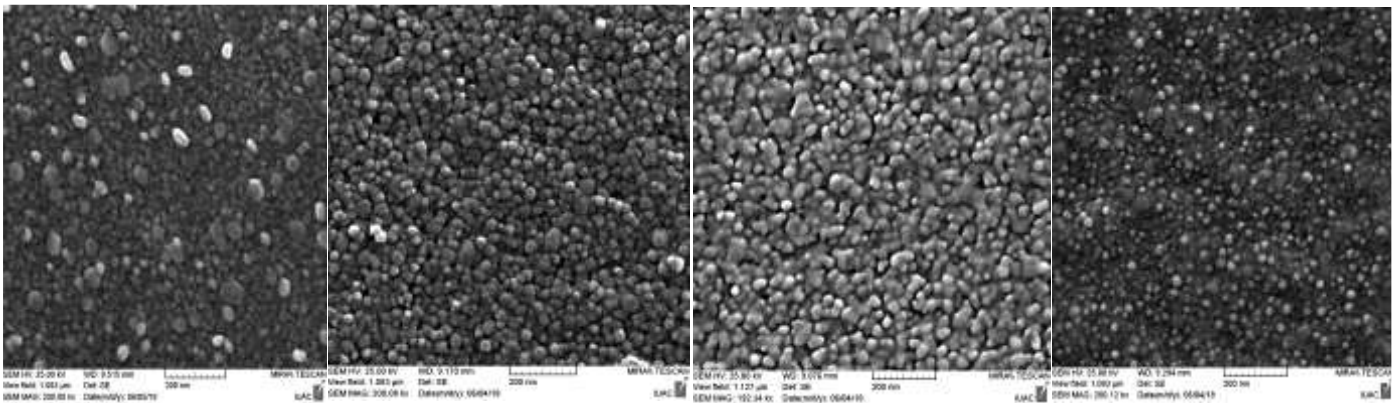

Figure 2: SEM Images of (a) Undoped ZnO (b) 1.5% AZO (c) 2% AZO (c) 2.5% AZO annealed at 500℃.

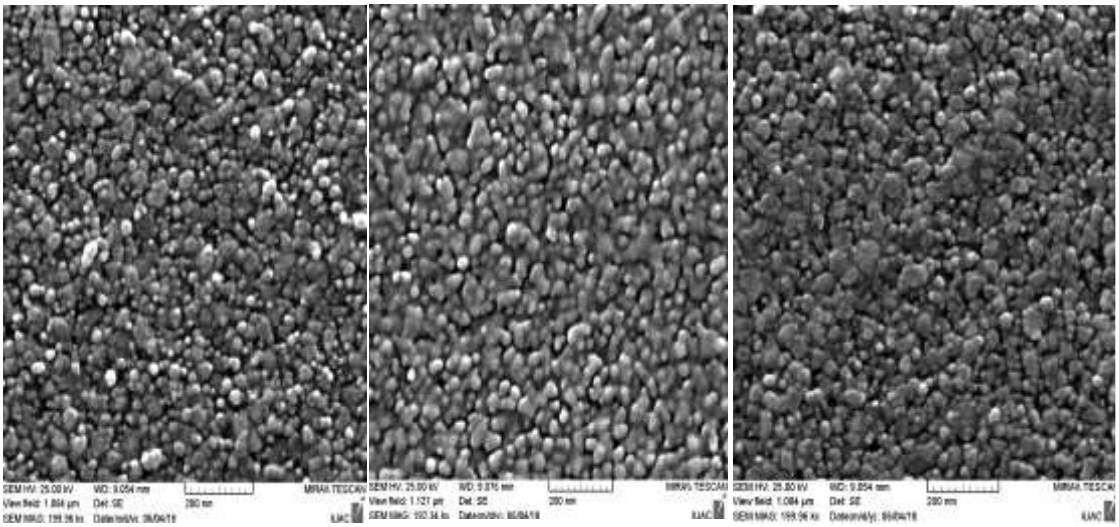

Figure3: SEM Image 2% AZO thin films annealed at three different temperatures viz. 500ºC, 600ºC and 700ºC.

The value of average particle size, calculated from FE-SEM images, changes from 30nm to 22 nm with increasing Al dopant concentration. As the ionic radii of zinc and aluminium are different, this difference disturb the grain growth due to compression stress and thus, particles those are forming a matrix become smaller with increasing Al concentration. Formation of matrix with smaller particles at base and the large particles lying on that matrix has been observed. The interfacial energy influence the formation and morphology of the thin films. Thus to investigate the effect of annealing, 2% AZO films annealed at three different temperature i.e. 500˚C, 600˚C and 700˚C. These results are shown in the Fig.3. A noticeable topographical transformation is observed in the films. The films annealed at 500˚C exhibit porous structure while with increase in annealing temperature films exhibit denser structure with a little increase in particle size. These changes can be attributed to the diffusion of atoms and change in their position in the crystal lattice caused by extra energy provided through the increased annealing temperature. The particle size calculated from SEM images are comparable with XRD crystallite size calculated by Scherrer's formula, but as expected XRD analysis under estimated the crystallite size. Similar results have been reported by other research groups , where with the increasing annealing temperature particles grow in size and the structures become more densely packed(Kuo et al., 2006).

3.3. Optical studies

The application of AZO thin films for TCOs require high transparency which is characterised via optical transmitance by UV–vis spectrophotometer within 300-800 nm wavelength range at room temperature. Fig4.(a) illustrates the optical transmitance of ZnO and AZO thin films deposited on corning glass substrate. It is obsereved that all the deposited thin films exihibit high transparency (above 78%) in the visible region. The increasing Al content raised the transmitance and the rise is more prominent at lower wavelenths.

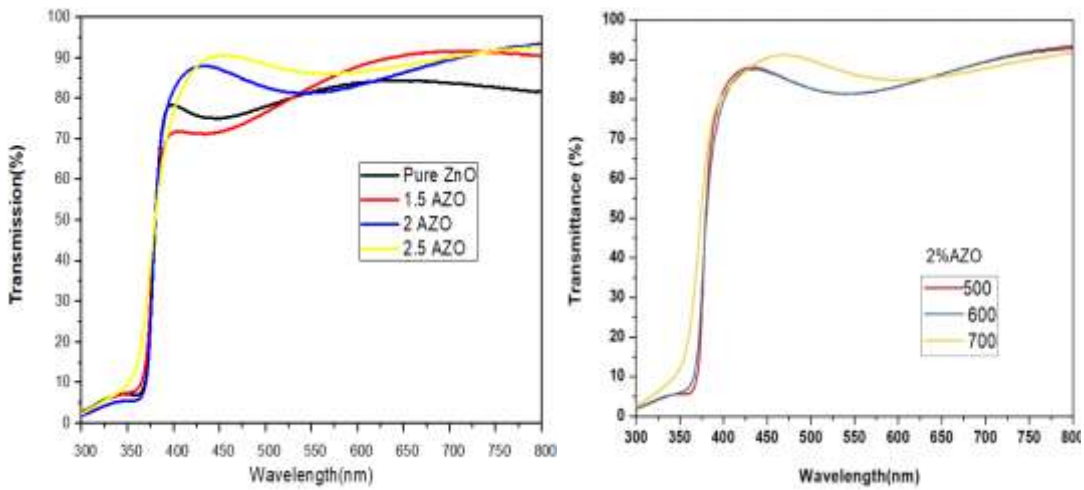

Figure 4: Transmission curve of thin films (a) 2% AZO thin films annealed at different annealing temperature (b) increasing Al concentration annealed at 500ºC.

The electronic transition from the valance band to the conduction band is responsible for this change at lower wavelenths. 90% Transmitance has been attained for 2.5% AZO films, annealed at 700℃ in oxygen environment. It is clearly observerd that the increase in Al doping content induces improvement in transparency of the host and make the AZO thin films a promising candidate for the transparent conducting application. The absorption edge for the undoped ZnO thin film is located ~370 nm. A blue shift is observerved in the absorption edge with increasing Al concentration and the absorption edge for the 2.5% AZO thin film is located near 355 nm. This shift in the absorption edge due to Al doping can be correlated with the optical band gap widening. Fig4.(b) illustrates optical tramitance of 2% AZO thin films annealed at three different temperatures viz. 500ºC, 600ºC and 700ºC. As the

annealing temperature increase, absorption edge shifts towards the lower wavelength which may also be attributed to enhancement in the crystalinity of annealed thin films, such results are also supported by the XRD and SEM observations.

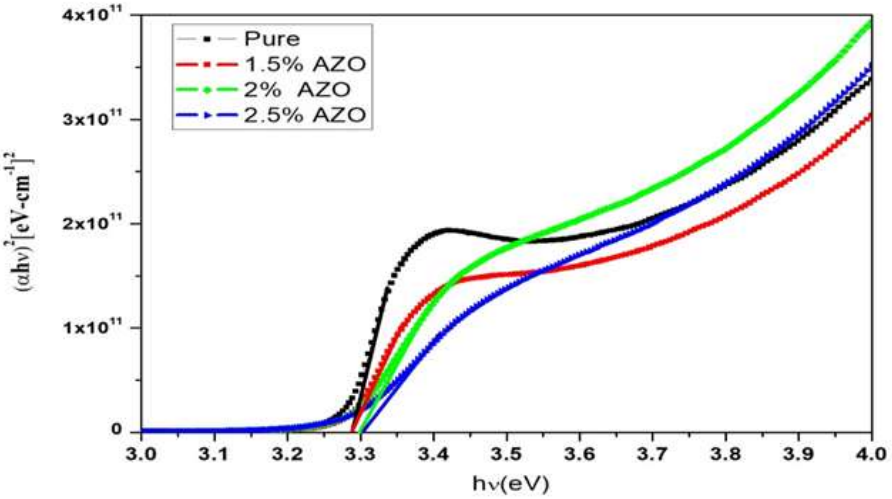

Figure5: Tauc plot for different doping concentration AZO thin films Annealed at 700ºC. (Optical Studies)

AZO thin films has a direct allowed transition similar to ZnO thin films. The optical band gap of the deposited ZnO and AZO thin films is estimated by employing the Tauc's plot(Tauc, Grigorovici, & Vancu, 1966)

$$\alpha h\nu \approx C(h\nu - E_g)^{1/2}$$

where, C is a constant , α is the absorption coefficient, $h\nu$ is the photon energy and 1/2 is for the direct transitions. E_g is the optical band gap and obtained by the extrapolated linear part of $(\alpha h\nu)^2$ versus $h\nu$ curve which coincide with the energy axis. Further the optical band gap is found to depend on different factors such as crystallite size, presence of strain in the films and carrier concentration(Joshi et al., 2016). Fig 5 shows the bandgap E_g values, for the different Al doping concentration, are obtained by plotting $(\alpha h\nu)^2$ versus $h\nu$ and are tabulated in Table 2. The obtained band gap values for the thin films are less than the bulk ZnO (3.37 eV). The difference in thickness and induced stress could be the reason for this change in comparison to the bulk ZnO.

Table2: Optical band gap of thin films.

Al Conc. /Anneling temp.	Undoped ZnO	1.5AZO	2AZO	2.5AZO
500°C	3.278	3.273	3.289	3.295
600°C	3.291	3.280	3.291	3.301
700°C	3.292	3.288	3.331	3.297

An increse in E_g value is observed with the increase in Al concentration in the AZO thin films. A further increse in the band gap is observed with the increasing anealing temperature. The 2% AZO thin films annealed at 700º C show the maximum band gap of 3.331 eV. The earlier reports show that the compressive stress and decrease in crystallite size, with an increase in Al concentration, causes the blue shift in the optical band gap. This observation is supported by XRD patteren. The observed band-gap widening may be attributed to the alterations in the band structure of undoped ZnO due to the doping of Al, which is well described by Burstein-Moss theory(Burstein, 1954). According to BM effect , the doping of Al^{3+} in Zn^{2+} provides an additional free elctoron, these free electrons occupy the unoccupied lowest levels in the bottom of conduction band. Due to this, the fermi level pushed higher and moves in the conduction band. By Pauli Exclusion Principle these states are prevented to be doubly occupied and consequently the increase in the energy is required for the electron excitation to higher energy state. Thus, in our present study the observed shift in the band gap may be due to the combined outcome of compressive stress and BM effect. The observed band gap widening is may be due to the effect of decrease in oxygen vacancies as annealing is carried out in oxygen envirenment.

3.4 Electrical Transport Studies

The electrical transport properties of the deposited thin films are measured by plotting the I-V charcteristics shown in figure. The results illustrates linear I-V curve and confirm that all the films have ohmic behaviour. The resistivity, ρ of the undoped ZnO and AZO thin films were calculated from the I-V curve using the equation:

$$\rho = \left(\frac{V}{I}\right)\frac{wt}{l}$$

Where, V is applied voltage, I is the measured current, w is electrode width, t is thickness of the film and l the distance between electrodes. Figure 6 shows the I-V characteristic of the thin film samples, annealed at 700ºC, with increasing Al dopant concentration.

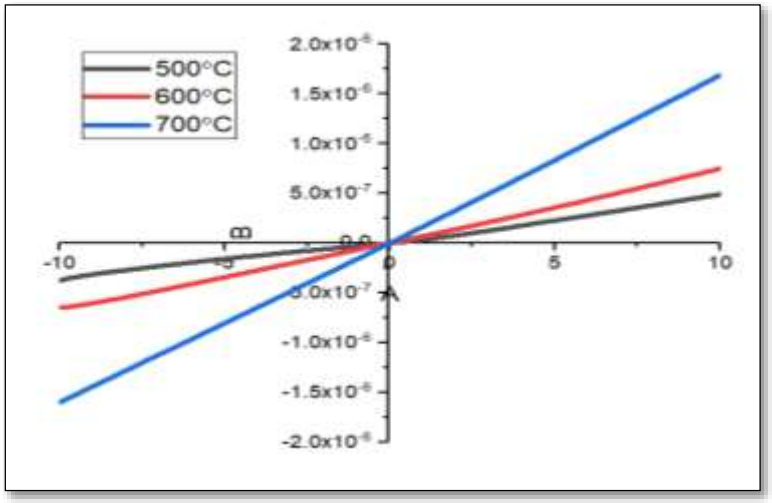

Figure6: IV curve for different doping concentration AZO thin films Annealed at 700ºC.

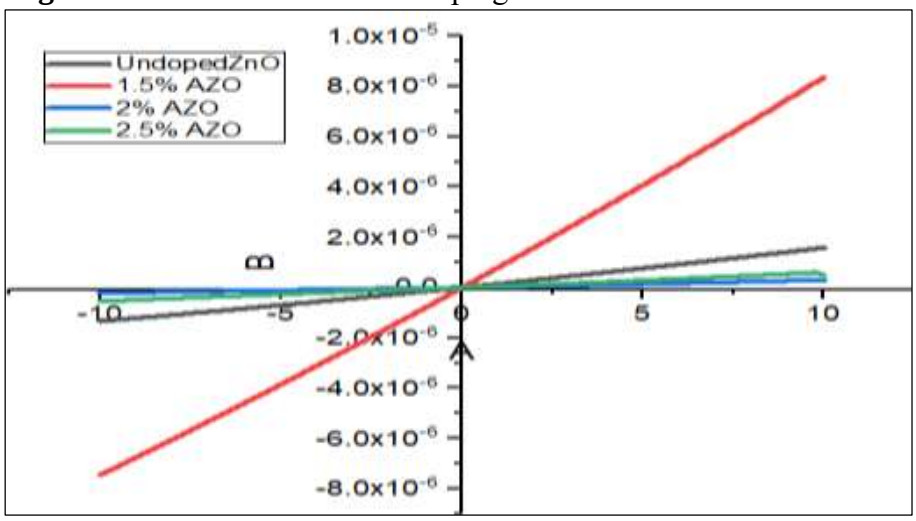

Figure7: IV curve for 2% AZO thin films annealed at three different temperatures viz. 500ºC, 600ºC and 700ºC.

The resistance of the thin films is in range of 108-109Ω. The calculated value are 2.54×108Ω, 1.7×108 Ω, 4.3×108 Ω and 2.7×109 Ω for undoped, 1.5AZO, 2AZO and 2.5AZO thin films respectively. The decrease in the resistivity could be observed for 1.5AZO thin film and this value increase with further increased in Al concentration for 2.5AZO thin film. The decreament in the resisitivity values may be attributed to the increase in the carrier concentration due to the free donar electrons from dopant atoms. The similar results are observed by other research groups. The increament in resistivity value, in case of 2.5AZO thin films, may results due to the deterioration of the crystallinity and lower crystal oreintation along c-axis, which is evident from the XRD pattern.

Figure 7 shows the effect of annealing temperature on resistivity of 2AZO thin films with increasing temperature. The values obtained from the curve are 4.68×10^{9} Ω, 2.71×10^{9} Ω and 4.3×10^{8} Ω for 2AZO thin film annealed in oxygen environment at 500ºC, 600ºC and 700ºC respectively. The results shows that the electrical resistivity value decreases with rise in temperature. This decrease can be related by the enhancement in the crystallinity with

increasing temperature. Annealing in the oxygen environment can contribute to the increment in carrier concentration which in turns reduce the resistivity(Lee & Park, 2004). At the elevated temperatures the particle merge together causing the densification in the films that results in the reduced oxygen adsorption on the grain boundaries. The increase in the conductivity can also be explained by the reduced carrier trapping due to annealing. The crystalline order of poly crystalline structure is limited to small regions known as grains. The atomic arrangement on the grain boundaries are not as much of ordered than inside the grain. This type of arrangement are believed to attract the conduction electrons and trap them near the grain boundaries, where the oxygen atoms also get accumulated. This whole condition generate a depletion region near to the grain boundaries and confine the flow of electrons from one grain to other. With increasing annealing temperature oxygen desorption which is believed to be a significant factor that improves electron mobility which in turns increase the conductivity of the thin films

4. CONCLUSIONS

In the present study, undoped ZnO and AZO thin films were successfully deposited on corning glass substrate by employing simplistic sol-gel spin coating technique. The study throws a light on the induced transformations due to effect of variation of Al dopant concenration and annealing temperature on the overall structural, morphological optical and electrical transport properties of the deposited thin films. Structural studies show that in comparision to the undoped ZnO thin films, improvement in the crystallinity for 1.5% and 2% AZO thin films has been observed and that on contrary the further increase in Al concentration for 2.5% AZO thin films, results in degaradation of structure of the films. The evolution in the grain size has been observed due to the effect of Al dopant concentration and annealing temperature. The morphological studies show the uniform distribution of the nano-sized grains in the thin films. The optical transparency is enhanced with Al doping and transmittance of the deposited thin films lies between 75 to 90%. The optical band gap, calculated from the Tauc plot method, is found to increase from 3.281 eV to 3.292 eV as Al concenteration changes from undoped ZnO to 2.5% AZO thin films, annealed at 500ºC in oxygen environment. The maximum value for the band gap of 3.331 eV is obtained for the 2% AZO thin film annealed at 700ºC. The observed augmentation in the forbidden energy range is a combined effect of intrinsic comperessive stress and BM effects. A significant band gap widening observed due to the presence of dopant which is further incresed for the annealed thin films. The electrical property is changed with annealing temperature. By the present investigation, we can conclude that the structural, morphological, optical and electrical properties of the thin films are influenced by the Al dopant concentration and annealing. Thus, with suitable alteration in Al concentration and annealing in oxygen environment at different temperatures, the characteristic properties can be tailored for the various applications.

5.ACKNLOWLEDGMENTS

Authors are grateful to the Director, Inter University Accelerator Centre, New Delhi for providing support throughout the experimental work. Authors are also thankful to Dr. S.A. Khan for experminetal support in FE-SEM invegstigation and Dr. Mukesh Rawat for the critical reading of the manuscript. One of the authors (RS) is also thankful to UGC for providing the financial the financial support under the scheme of Ph.D. student fellowship.

References

Barón-Miranda, J. A., Calzadilla, O., San-Juan-Hernández, S., Diez-Pérez, I., Díaz, J., Sanz, F., … Caballero-Briones, F. (2017). Influence of texture on the electrical properties of Al-doped ZnO films prepared by ultrasonic spray pyrolysis. *Journal of Materials Science: Materials in Electronics*, *29*(3), 2016–2025. https://doi.org/10.1007/s10854-017-8113-x

Brinker, C. J., & Scherer, G. W. (1990). Sol-gel sciences. *The Processing and the Chemistry of Sol-Gel Processing*.

Burstein, E. (1954). Anomalous optical absorption limit in InSb. *Physical Review*, *93*(3), 632.

Fiat Varol, S., Babür, G., Çankaya, G., & Kölemen, U. (2014). Synthesis of sol-gel derived nano-crystalline ZnO thin films as TCO window layer: Effect of sol aging and boron. *RSC Advances*, *4*(100), 56645–56653. https://doi.org/10.1039/c4ra11324a

Gautam, S. K., Singh, R. G., Kumar, V. V. S., & Singh, F. (2015). Giant enhancement of the n-type conductivity in single phase p-type ZnO: N thin films by intentionally created defect clusters and pairs. *Solid State Communications*, *218*, 20–24.

Hosford. (2013). *Materials science*.

Jo, G. H., Kim, S. H., & Koh, J. H. (2018). Enhanced electrical and optical properties based on stress reduced graded structure of Al-doped ZnO thin films. *Ceramics International*, *44*(1), 735–741. https://doi.org/10.1016/j.ceramint.2017.09.240

Joshi, K., Rawat, M., Gautam, S. K., Singh, R. G., Ramola, R. C., & Singh, F. (2016). Band gap widening and narrowing in Cu-doped ZnO thin films. *Journal of Alloys and Compounds*. https://doi.org/10.1016/j.jallcom.2016.04.093

Kaur, G., Mitra, A., & Yadav, K. L. (2015). Influence of Beam Energy on the Properties of Pulsed Laser Deposited Al-Doped ZnO Thin Films. *IEEE Transactions on Nanotechnology*, *14*(5), 922–930. https://doi.org/10.1109/TNANO.2015.2463085

Kuo, S. Y., Chen, W. C., Lai, F. I., Cheng, C. P., Kuo, H. C., Wang, S. C., & Hsieh, W. F. (2006). Effects of doping concentration and annealing temperature on properties of highly-oriented Al-doped ZnO films. *Journal of Crystal Growth*, *287*(1), 78–84. https://doi.org/10.1016/j.jcrysgro.2005.10.047

Lee, J. H., & Park, B. O. (2004). Characteristics of Al-doped ZnO thin films obtained by ultrasonic spray pyrolysis: Effects of Al doping and an annealing treatment. *Materials Science and Engineering B: Solid-State Materials for Advanced Technology*, *106*(3), 242–245. https://doi.org/10.1016/j.mseb.2003.09.040

Li, J., Yang, D., & Zhu, X. (2017). Pretreating temperature controls on structural, morphological and optical properties of sol–gel ZnO thin films. *Materials Technology*, *7857*(November), 1–7. https://doi.org/10.1080/10667857.2017.1396775

Look, D. C., & Hemsky, J. W. (2000). native defects ref Residual Native Shallow Donor in ZnO, *82*, 2–5.

Malek, M. F., Mamat, M. H., Musa, M. Z., Soga, T., Rahman, S. A., Alrokayan, S. A. H., … Rusop, M. (2015). Metamorphosis of strain/stress on optical band gap energy of ZAO thin films via manipulation of thermal annealing process. *Journal of Luminescence*, *160*, 165–175. https://doi.org/10.1016/j.jlumin.2014.12.003

Nunes, P., Fortunato, E., Vilarinho, P., & Martins, R. (2001). Effect of different dopants on the properties of ZnO thin films, *3*, 1211–1213.

Park, S. K., Hwang, C., Ryu, M., Yang, S., Byun, C., Shin, J., … Im, S. (2009). Transparent and photo-stable ZnO thin-film transistors to drive an active matrix organic-light-emitting-diode display panel. *Advanced Materials*, *21*(6), 678–682.

Pat, S., Mohammadigharehbagh, R., Özen, S., Şenay, V., Yudar, H. H., & Korkmaz, Ş. (2017). The Al doping effect on the surface, optical, electrical and nanomechanical properties of the ZnO and AZO thin films prepared by RF sputtering technique. *Vacuum*, *141*. https://doi.org/10.1016/j.vacuum.2017.04.025

Pramod, N. G., & Pandey, S. N. (2014). Influence of Sb doping on the structural, optical, electrical and acetone sensing properties of In2O3 thin films. *Ceramics International*, *40*(2), 3461–3468.

Singh, R. G., Singh, F., Kumar, V., & Mehra, R. M. (2011). Growth kinetics of ZnO nanocrystallites: Structural, optical and photoluminescence properties tuned by thermal annealing. *Current Applied Physics*, *11*(3), 624–630. https://doi.org/10.1016/j.cap.2010.10.013

Srinatha, N., Raghu, P., Mahesh, H. M., & Angadi, B. (2017). Spin-coated Al-doped ZnO thin films for optical applications: Structural, micro-structural, optical and luminescence studies. *Journal of Alloys and Compounds*, *722*, 888–895. https://doi.org/10.1016/j.jallcom.2017.06.182

Tauc, J., Grigorovici, R., & Vancu, A. (1966). Optical properties and electronic structure of amorphous germanium. *Physica Status Solidi (B)*, *15*(2), 627–637.

Thandavan, T. M. K., Gani, S. M. A., Wong, C. S., & Nor, R. M. (2015). Enhanced photoluminescence and Raman properties of Al-doped ZnO nanostructures prepared using thermal chemical vapor deposition of methanol assisted with heated brass. *PLoS ONE*, *10*(3). https://doi.org/10.1371/journal.pone.0121756

Venkataraj, S., Ohashi, N., Sakaguchi, I., Adachi, Y., Ohgaki, T., Ryoken, H., & Haneda, H. (2007). Structural and magnetic properties of Mn-ion implanted ZnO films. *Journal of Applied Physics*, *102*(1). https://doi.org/10.1063/1.2752123

Yilmaz, M., Tatar, D., Sonmez, E., Cirak, C., Aydogan, S., & Gunturkun, R. (2016). Investigation of Structural, Morphological, Optical, and Electrical Properties of Al Doped ZnO Thin Films Via Spin Coating Technique. *Synthesis and Reactivity in Inorganic, Metal-Organic and Nano-Metal Chemistry*, *46*(4), 489–494. https://doi.org/10.1080/15533174.2014.988795

Yu, D., Yang, Y.-Q., Chen, Z., Tao, Y., & Liu, Y.-F. (2016). Recent progress on thin-film encapsulation technologies for organic electronic devices. *Optics Communications*, *362*, 43–49.